ELSEVIER

Biophysical Chemistry 111 (2004) 63–71

Biophysical Chemistry

www.elsevier.com/locate/bpc

Binding mode of cationic monomer and dimer porphyrin with native and synthetic polynucleotides studied by polarized light spectroscopy

Jin-Ok Kim[a], Young-Ae Lee[a], Biao Jin[a], Taegi Park[a], Rita Song[b], Seog K. Kim[a,*]

[a] *Department of Chemistry, Yeungnam University, Dae-dong, Kyoungsan City, Kyoung-buk 712-749, Republic of Korea*
[b] *Department of Chemistry, Ewha Woman's University, Seoul 120-750, Republic of Korea*

Received 17 January 2004; received in revised form 20 April 2004; accepted 22 April 2004
Available online 18 May 2004

Abstract

Binding properties of the tricationic porphyrin monomer with a phenolic substituent at the periphery and the porphyrin dimer conjugated with hydrophilic triethylene glycol were investigated in this study using absorption and polarized spectroscopy, namely, circular dichroism (CD) and linear dichroism (LD). The spectral properties of the porphyrin monomer, when complexed with polynucleotides, were essentially the same as that of the well-known *meso*-tetrakis(*N*-methylpyridiniumyl)porphyrin, indicating that the substitution at one peripheral pyridiniumyl ring did not affect the binding mode. When the porphyrin dimer formed a complex with poly[d(G-C)$_2$], a negative CD band and a negative LD^r spectrum were apparent in the Soret absorption region, with its LD^r magnitude significantly smaller than that in the DNA absorption region. As the complex was stabilized over time, the intensity of the negative CD band and the negative LD^r increased. These observations indicated that one of the porphyrin moieties of the dimer intercalated initially and than the other one also intercalated consecutively within a few hours. In the porphyrin dimer–poly[d(A-T)$_2$] complex case, a bisignate CD was apparent and remained for at least 12 h, indicating that the porphyrins are stacked along the polynucleotide stem even at a very low [porphyrin]/[DNA base] ratio. A wavelength-dependent and time-dependent LD^r of this complex suggests that the porphyrin molecular plane tilts strongly relative to the polynucleotide helix axis. The spectral properties of the porphyrin dimer–DNA complex are similar to those of the porphyrin dimer–poly[d(G-C)$_2$] complex. However, some of the porphyrin moieties were located at the groove, which was evident by some positive characters in the CD and LD^r spectra at the short wavelength in the Soret band.

Keywords: Porphyrin; DNA; Circular dichroism; Linear dichroism; Intercalation; Groove binding

1. Introduction

Porphyrin derivatives have been an interesting DNA probe for various binding modes that depend on the nature of the porphyrin ring, the periphery substituent group, and the central metal (see Refs. [1–3] for reviews). In addition, the nature of the DNA bases also affects the binding mode of porphyrins. In general, three binding modes for the porphyrin derivatives–DNA complex have been accepted, namely, intercalation, outside stacking, and outside random binding. The groove binding mode was also suggested from recent circular dichroism (CD) and linear dichroism (LD) studies [4–12].

Intercalation and outside binding may be influenced also by the charge on the porphyrin core [4,5]. Intercalation binding mode favors GC base pairs, while the outside binding prefers AT base pairs. The outside binding mode, which is characterized by a bisignate strong CD band in the Soret absorption band, can be classified as "extensive stacking" (or extensive assembly) and "moderate stacking" (or modest aggregation) mode [13,14]. An extensive self-stacked form is favored at a high [porphyrin]/[DNA base] ratio and at a high salt concentration, while porphyrin stacks moderately at a low

* Corresponding author. Tel.: +82-53-810-2362; fax: +82-53-815-5412.
E-mail addresses: seogkim@yu.ac.kr, seogkim@yumail.ac.kr (S.K. Kim).

0301-4622/$ - see front matter © 2004 Elsevier B.V. All rights reserved.
doi:10.1016/j.bpc.2004.04.004

[porphyrin]/[DNA base] ratio and at a low salt concentration [15,16]. The extent of self-aggregation of porphyrin on the DNA template is also affected by the nature of the central metal ion and the properties of the substituent groups on the periphery of the porphyrin [15,16]. The shape of the bisignate CD of self-assembled porphyrins depends on the order of the base sequence [17]. Recently, the location of the stacking has been suggested to be at the major groove of DNA [18].

In this study, the binding properties of monomeric and dimeric porphyrins (Scheme 1) to DNA, poly[d(A-T)$_2$], and poly[d(G-C)$_2$] were investigated, using polarized light spectroscopies. The porphyrin dimer is, at least in part, stacked in aqueous solution, whereas the porphyrin monomer is not, thereby allowing comparison of the binding mode of porphyrin on the DNA template between already stacked porphyrin and unstacked ones. Poly[d(A-T)$_2$] and poly[d(G-C)$_2$] were chosen because they provide contrasting binding sites for porphyrin at a low [porphyrin]/[DNA base] ratio, namely, minor groove and intercalation site, respectively [11,12].

2. Experimental

2.1. Synthesis of porphyrin dimer

A procedure to synthesise porphyrin dimer (porphyrin 3 in Scheme 1) and monomer (porphyrin 4) is outlined in Scheme 1. The starting porphyrin 1, 5-[4-(ethylcarbonyl)oxy]-phenyl]-10,15,20-tris(4-pyridyl)porphyrin, was prepared according to the procedures reported in the literature [19]. In order to obtain porphyrin 2, triethylene glycol ditosylate was added to a solution of porphyrin 1 in DMF in the presence of NaOH. The following spectroscopic results were obtained from the reactant porphyrin 2: yield 34%; ^{1}H nuclear magnetic resonance (NMR) ($CDCl_3$, δ): 9.10 (d, 6*H*, 2,6-pyridyl), 8.89 (m, 8*H*, β-pyrrol), 8.21 (d, 6*H*, 3,5-pyridyl), 8.18 (d, 2*H*, 2,6-phenyl), 7.84 (d, 2*H*, tosyl), 7.25 (d, 2*H*, tosyl), 7.30 (d, 2*H*, 3,5-phenyl), 4.44 (m, 2*H*, CH_2), 4.27 (m, 2*H*, CH_2), 4.07 (m, 2*H*, CH_2), 3.77–3.86 (m, 6*H*, CH_2), 2.45 (s, 3*H*, tosyl-CH_3), and −2.85 (s, 2*H*, NH pyrrol).

The porphyrin 1 and porphyrin 2 mixture in DMF in the presence of 1 M KOH was stirred for several hours and

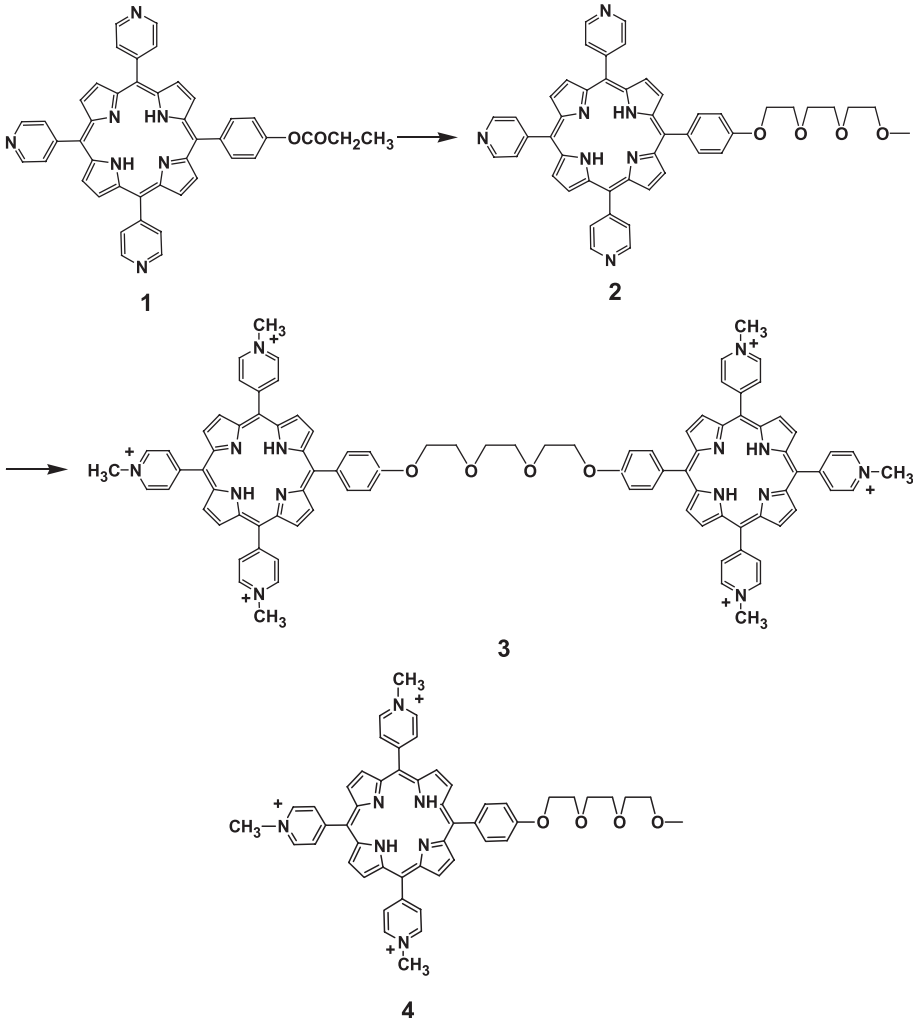

Scheme 1. Synthetic procedure and chemical structure of the porphyrins.

recrystallization followed. The crystal was redissolved in DMF and methylated with great excess of methyl iodide to give the final product (porphyrin 3). The following spectroscopic results were obtained from the reactant porphyrin 3: yield 35%; ^{1}H NMR (DMSO-d_6, δ): 9.50 (d, 12*H*, 2,6-pyridiniumyl), 9.31 (m, 16*H*, β-pyrrol), 9.01 (d, 12*H*, 3,5-pyridiniumyl), 8.19 (d, 4*H*, 2,6-phenyl), 7.45 (d, 4*H*, 3,5-phenyl), 4.83 (s, 18*H*, N^+-CH_3), 4.52 (m, 4*H*, CH_2), 4.17 (m, 4*H*, CH_2), 4.02 (m, 4*H*, CH_2), and −2.89 (s, 4*H*, NH pyrrol). Porphyrin 4 was obtained by direct methylation of porphyrin 2 by an excess amount of methyl iodide.

The purity of the porphyrins obtained from every step was ensured by recrystallization and chromatography performed several times (silicagel, CH_2Cl_2-EtOH, 96/4). Elemental analyses were performed at the Korea Basic Science Institute (Seoul, South Korea). ^{1}H NMR spectra were measured on a Bruker 250 MHz spectrometer. ES-MS measurements were performed by a HP 5989A equipped with HP 59987A as an electron spray source. Tri(ethylene glycol), *p*-toluenesulfonyl chloride, 4-hydroxybenzaldehyde, pyrrol, 4-pyrisinecarboxaldehyde, and iodomethane purchased from Aldrich (Seoul, South Korea) were used without further purification.

2.2. Others materials

Calf thymus DNA (referred to as DNA), poly[d(G-C)$_2$], and poly[d(A-T)$_2$] were purchased from Amersham Pharmacia Biotech (New Jersey, USA). Polynucleotide was dissolved in 5 mM cacodylate buffer solution at pH 7.0, containing 100 mM NaCl and 1 mM EDTA, followed by several rounds of dialysis against 5 mM cacodylate buffer solution, pH 7.0, at 4 °C. A 5-mM cacodylate buffer solution was used throughout this study. The concentrations of DNA were determined using the extinction coefficients: $\varepsilon_{258\ nm} = 6700\ cm^{-1}\ M^{-1}$, $\varepsilon_{254\ nm} = 8400\ cm^{-1}\ M^{-1}$, and $\varepsilon_{262\ nm} = 6600\ cm^{-1}\ M^{-1}$ for DNA, poly[d(G-C)$_2$], and poly[d(A-T)$_2$] in nucleobase, respectively. Those for the porphyrin monomer 4 and dimer 3 were measured to be $\varepsilon_{425\ nm} = 92{,}000\ cm^{-1}\ M^{-1}$ and $\varepsilon_{423\ nm} = 212{,}000\ cm^{-1}\ M^{-1}$, respectively. The concentration of both monomer and dimer porphyrins used in this study indicates a concentration of the porphyrin chromophore. Therefore, 10 μM dimer denotes 10 μM porphyrin concentration, which is equivalent to the 5-μM dimer molecule. Since the appearance of spectra for the porphyrin–DNA complex is affected by the order of mixing [20], aliquots of concentrated porphyrin were always added last to the DNA solution.

2.3. Methods

Absorption spectra were recorded on either a Jasco V550 (Tokyo, Japan) or a Cary 500 (Varian, Australia). CD is induced for achiral DNA-bound drugs due to the interaction of the drug's electric transition moments and chirally arranged DNA base transition moments. The induced CD is sensitive to the drug's environment and is used to probe the interaction with DNA [20,21]. An apparent bisignate CD in the Soret band is characteristic of porphyrin that is stacked or assembled along the DNA stem [17], while positive CD band(s) has been assigned for those bound to the grooves [6,11]. A negative CD band is generally accepted as a diagnostic for the intercalated porphyrin [12,21].

LD is the difference in absorption spectrums for the light polarized parallel and perpendicular to the orientation of the molecule [22,23]. Measured LD was divided by an isotropic absorption spectrum to give a reduced LD (LD^r), which is related to angle α between the transition moment of DNA-bound drugs and the local DNA helix axis:

$$\mathrm{LD}^{\mathrm{r}}(\lambda) = \frac{\mathrm{LD}(\lambda)}{A_{\mathrm{iso}}(\lambda)} = \frac{3S}{2}(3\cos^2\alpha - 1)$$

where the orientation factor *S* is the measure of the ability of the DNA sample to orient in the flow. The angle α is calculated from LD^r value by assuming an effective angle of 86° at 260 nm for the DNA bases of the porphyrin–DNA complex with respect to the DNA helix axis [24]. The contributions of the porphyrin absorbance in this region are small because the extinction coefficient of the porphyrin at 260 nm is very small. Furthermore, the mixing ratios for all complexes are less than 0.1. Indeed, the values of the angle α were mixing ratio-independent, justifying our assumption. For the degenerated transition moments, the tilt angle is obtained by replacing $\cos^2\alpha$ with $1/2\cos^2\beta$ [25]. CD and LD spectra were recorded on a Jasco J 715 spectropolarimeter. For LD measurement, a flow-orienting Couette cell device as described by Nordén and Seth [26] was used. The flow rate was 600 rpm and the path length was 0.1 cm. All measurements were performed at an ambient temperature.

3. Results

The spectral characteristics of porphyrins 4 and 3 complexed with DNA, poly[d(A-T)$_2$], and poly[d(G-C)$_2$] at low [porphyrin]/[DNA base] ratios (<0.1) were essentially invariant of the mixing ratio. Therefore, the spectra shown in this article represent those recorded at various mixing ratios under 0.1.

3.1. Spectral properties of porphyrin monomer 4 complexed with DNA, poly[d(A-T)$_2$], and poly[d(G-C)$_2$]

The interaction of *meso*-tetrakis(*N*-methylpyridiniumyl)-porphyrin (TMPyP) with various natural and synthetic polynucleotides has been extensively investigated by CD and LD at low [porphyrin]/[DNA base] ratios [10–12,17,18]. The porphyrin monomer investigated in this study is structurally related with TMPyP, except for one functionalized phenyl substituent at periphery of the porphyrin ring. The absorption spectrum of porphyrin 4 monomer (Scheme 1) complexed with DNA, poly[d(A-

$T)_2$], and poly[d(G-C)$_2$] in the Soret region is compared with that of DNA-free porphyrin in Fig. 1A. At a low mixing ratio, porphyrin monomer 4 exhibits red shift and hypochroism upon binding to polynucleotides, as other typical DNA-binding drugs do. In the presence of poly[d(G-C)$_2$], red shift and hypochroism are most pronounced at 24 nm and 42%. The spectral change in the presence of DNA is 13 nm and 39%. In the presence of poly[d(A-T)$_2$], that was 8 nm and 7%. This result is similar to that observed for the TMPyP polynucleotide complexes [11]. The appearance of CD spectrum in the Soret band of porphyrin 4 in the presence of various polynucleotides (Fig. 1B) is similar to those of TMPyP. A negative CD band centered at 443 nm is apparent in the presence of either DNA or poly[d(G-C)$_2$]. On the other hand, two positive bands at 423 and 435 nm for poly[d(A-T)$_2$] complex are pronounced. The changes in absorption and CD spectrum in the DNA absorption region represent the conformation change of either DNA or porphyrin 4, or both, which cannot be properly analyzed at this stage; therefore, the spectrum in this region is not shown.

The LD^r spectrum of porphyrin 4 complexed with DNA, poly[d(A-T)$_2$], and poly[d(G-C)$_2$] in the DNA absorption region and the Soret region is shown in Fig. 1C. The magnitude of LD^r in the Soret region is strongly dependent on the wavelength for all complexes as it was observed in the TMPyP case [11], suggesting that the geometry of porphyrin 4 relative to the DNA is complicated. However, the LD^r magnitude in the Soret region of porphyrin 4–DNA and porphyrin 4–poly[d(G-C)$_2$] complexes was larger than that of the DNA region, indicating that both the *x* and *y* directions of the porphyrin system are almost perpendicular to the DNA

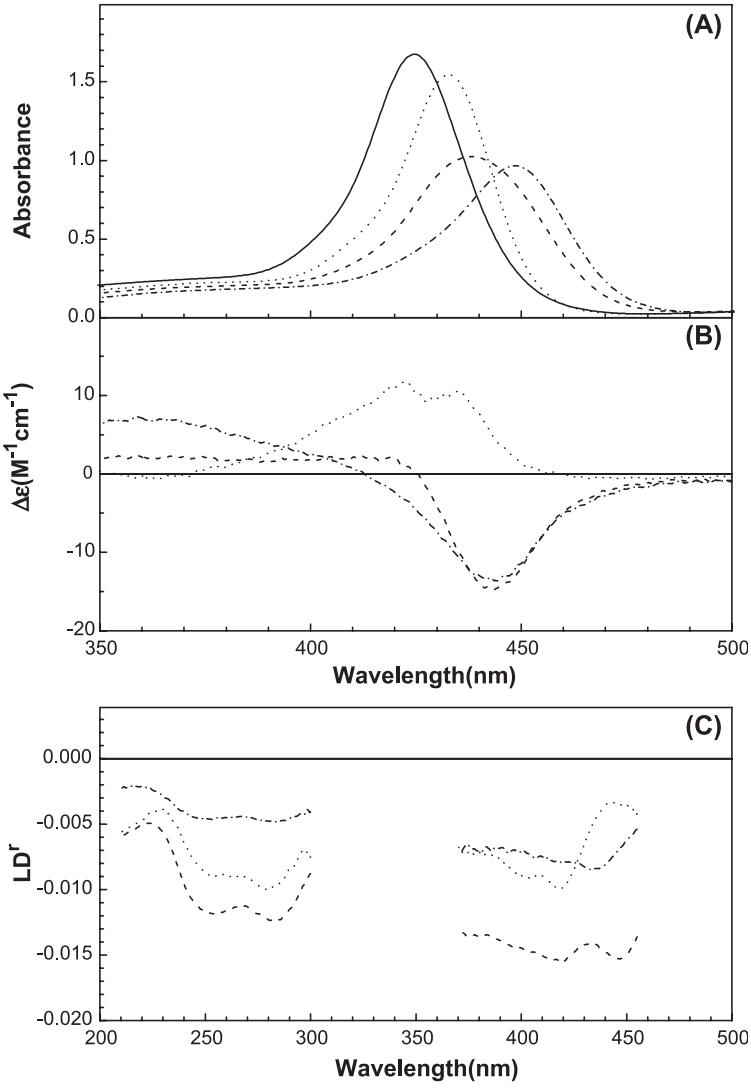

Fig. 1. Absorption (A), CD spectrum (B), and LD^r (C) spectrum of the porphyrin monomer 4 in the presence of DNA (dashed curve), poly[d(A-T)$_2$] (dotted curve), and poly[d(G-C)$_2$] (dash-dotted curve). LD^r spectra of the latter two complexes are enlarged four times for easy comparison. Absorption spectrum of porphyrin 4 in the absence of the polynucleotide is marked as a thick solid curve in panel (A). [Polynucleotide] = 200 μM in base; [porphyrin 4] = 16 μM. Note that the spectral properties at the lower mixing ratios are essentially the same as that shown here.

helix axis [22,23]. In the porphyrin 4–poly[d(A-T)$_2$] complex case, wavelength dependence is the largest, although the sign of the LD^r signal in the entire Soret region is negative. The LD^r magnitude at short wavelength regions in the Soret band is comparable with that in the DNA absorption region, while it is significantly smaller at a long wavelength, suggesting that the plane of the porphyrin molecule is tilted strongly relative to the DNA helix axis. Similar wavelength-dependent LD^r have been observed for the TMPyP–poly[d(A-T)$_2$] complex [7,10,11].

3.2. Spectral properties of the porphyrin dimer 3–DNA complex

The change in the absorption spectrum of the porphyrin dimer 3 (Scheme 1) upon binding to DNA is quite different from that of porphyrin 4 (Fig. 2A). The extent of hypochroism and red shift is significantly less pronounced than the porphyrin monomer 4–DNA complex being 10 nm and 16%, respectively. After 12 h of mixing, a small increase in absorbance and an additional 1–2 nm red shift was observed. In contrast with porphyrin 4, when porphyrin 3 formed a complex with DNA, a bisignate CD spectrum with a positive band at ca. 407 nm and a negative band at ca. 436 was initially apparent (Fig. 2B). As time lapsed, both the positive maximum and the negative minimum shifted 8 and 4 nm to a long wavelength, respectively. The intensity of the final CD is more than twice the extent compared to the initial measurement. An isodichroic point was observed during the change in the absorption spectrum of the porphyrin 3–DNA complex while it did not appear in the CD spectrum, suggesting that the change in porphyrin 3 conformation is

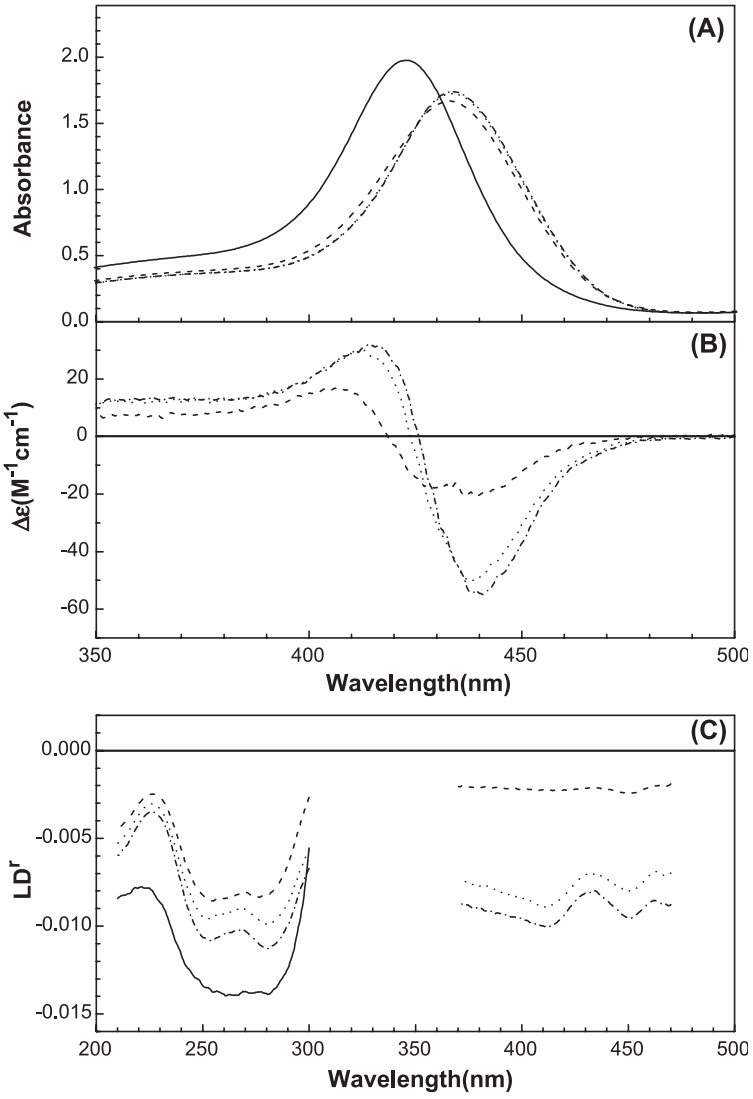

Fig. 2. Absorption (A), CD spectrum (B), and LD^r spectrum (C) of the porphyrin dimer 3–DNA complex, immediately after mixing (dashed curve) and 3 h (dotted curve) and 12 h (dash-dotted curve) after mixing. In panel (A), the absorption spectrum of the DNA-free porphyrin 3 appears as a thick solid curve. The LD^r spectrum of DNA in the absence of porphyrin is marked as a thick solid curve in panel (C). The spectral properties after 12 h remain essentially the same. [DNA] = 200 μM in base; [porphyrin 3] = 9.4 μM; hence, the porphyrin concentration corresponds to 18.8 μM.

not a simple two-step process. The LD^r spectrum of the porphyrin 3–DNA complex is shown in Fig. 2C. The initial magnitude of negative LD^r in the Soret band, which was recorded immediately after mixing, is very small compared to that in the DNA absorption region and is constant in the entire Soret band. This suggests that both the x and y transitions of porphyrin are significantly tilted relative to the DNA helix axis, and the extent of the tilts for both transitions was similar. Angle α between the transition moments along the porphyrin molecular plane and the DNA helix axis appeared to be 60.0°. However, the two transition moments of porphyrin in the Soret band are degenerated, and the constant LD^r value in the Soret band indicates that the degeneracy was not removed, Therefore, angle β should be a more reliable value, which was calculated to be 45.0°. The magnitude of LD^r in the Soret region increases with time and reaches its maximum after few hours of mixing. The final magnitude is comparable with that in the DNA absorption region, suggesting that the molecular plane of porphyrin is perpendicular with respect to the DNA helix axis. However, it is noteworthy that a positive contribution around 430–440 nm was apparent in the final LD^r spectrum of the porphyrin 3–DNA complex. The LD^r magnitude in the DNA absorption region right after mixing decreased to almost half of that in the absence of the porphyrin, suggesting that the ability of the orientation of the DNA decreases upon porphyrin binding. The decrease in orientability may due to local denaturation or, more likely, bending of the DNA at the porphyrin binding site. The LD^r magnitude in this region increased with time, but never recovered to the magnitude that was observed in the absence of porphyrin.

3.3. Spectral properties of the porphyrin dimer 3–synthetic polynucleotide complex

Upon association with poly[d(G-C)$_2$], porphyrin 3 exhibited a large red shift and hypochroism at 10 nm and 30.3%, respectively (Fig. 3A). Further red shift and a small

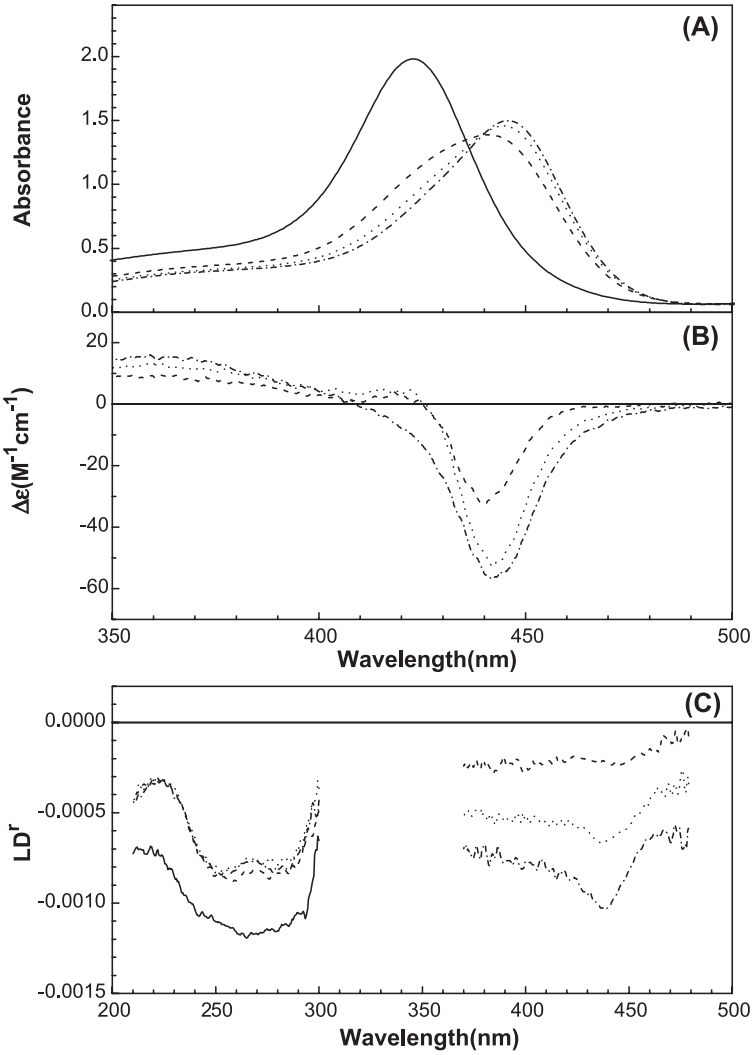

Fig. 3. Absorption (A), CD spectrum (B), and LD^r spectrum (C) of the porphyrin dimer 3–poly[d(G-C)$_2$] complex. The conditions and curve assignments are the same as in Fig. 2.

hyperchroism compared to that obtained from the initial complex were noticed as the time lapsed. Twelve hours after mixing, the red shift was 14 nm and the hypochroism was 24.7% compared to that in the absence of polynucleotide. A broad negative CD band in the Soret region was apparent for the porphyrin 3–poly[d(G-C)$_2$] complex (Fig. 3B), which is a diagnostic of porphyrin intercalation. The magnitude of this negative CD band increases with time so much so that the final magnitude is almost twice as much as that right after mixing. Fig. 3C depicts the LD^r spectrum of porphyrin 3–poly[d(G-C)$_2$] complex. At a glance, LD^r behavior of the porphyrin 3–poly[d(G-C)$_2$] complex seems to be similar to that of the porphyrin 3–DNA complex. However, the slow recovery of the LD^r magnitude in the DNA absorption region was not observed for the porphyrin 3–poly[d(G-C)$_2$] complex; the LD^r intensity decreased at the time of mixing and it did not recover. For the porphyrin 3–poly[d(G-C)$_2$] complex immediately after mixing, angle β is 44.6°. The shape of the LD^r spectrum at 12 h after mixing was essentially the same as that of the porphyrin monomer 4–poly[d(G-C)$_2$] complex. The LD^r magnitude in the entire Soret band of the final complex was larger than that in the DNA absorption region, indicating that both x and y transitions are perpendicular to the DNA helix axis and, therefore, suggest the intercalation of both porphyrin moieties [22,23]. A negative contribution in the LD^r spectrum around 440 nm was apparent, which is in contrast with that of the porphyrin 3–DNA complex.

Fig. 4 shows absorption, CD spectrum, and LD^r spectrum of the porphyrin 3–poly[d(A-T)$_2$] complex. In contrast with the porphyrin 3–DNA and–poly[d(G-C)$_2$] complex, the porphyrin 3–poly[d(A-T)$_2$] complex exhibited the smallest initial hypochroism and red shift in the absorption spectrum.

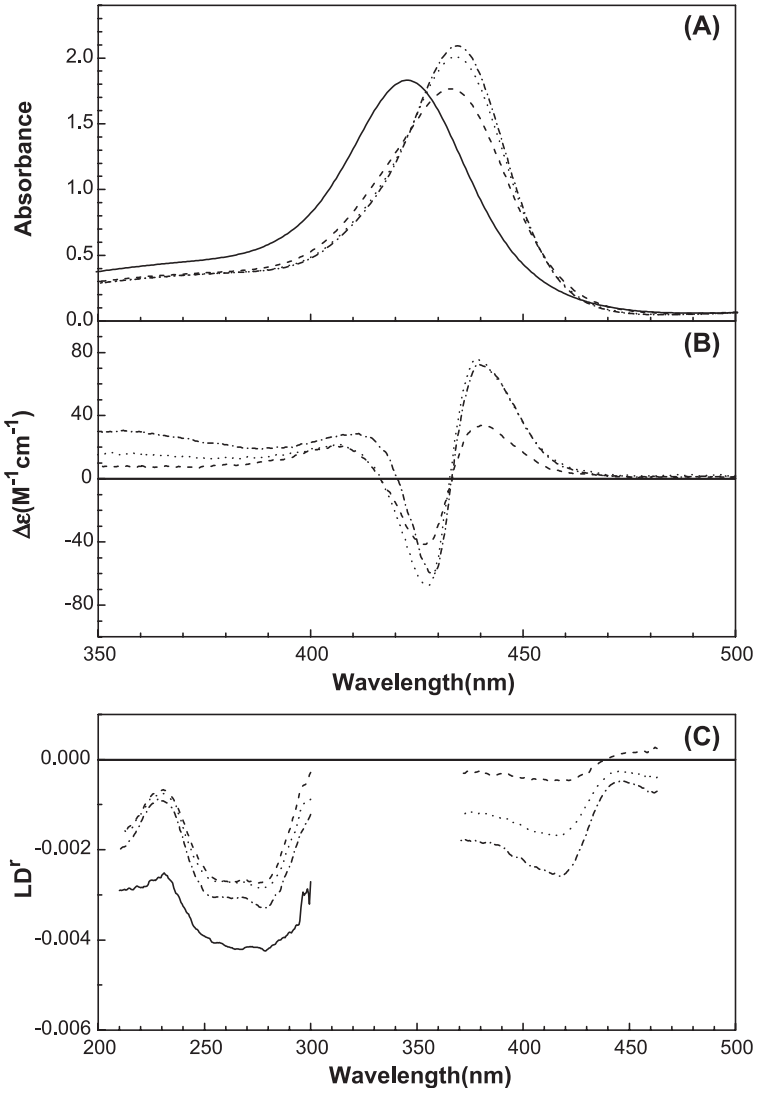

Fig. 4. Absorption (A), CD spectrum (B), and LD^r spectrum (C) of the porphyrin dimer 3–poly[d(A-T)$_2$] complex. The conditions and curve assignments are the same as in Fig. 2, except for porphyrin concentration, which is [porphyrin 3] = 8.6 μM; hence, the porphyrin concentration corresponds to 17.2 μM.

As the complex stabilized, the absorbance increased and the maximum shifted to the long wavelength by 10 nm. The apparent bisignate CD spectrum with its negative minimum at ca. 428 nm and positive maximum at ca. 441 nm (Fig. 4B) indicates that the porphyrins stack on the poly[d(A-T)$_2$] stem. The intensity of this bisignate CD increased as the complex stabilized. The wavelength dependence in the Soret band of the LD^r spectrum was the largest for the porphyrin–poly[d(A-T)$_2$] complex. Initially, the positive LD^r in the long wavelength edge in the Soret band was noticed (Fig. 4C) with a negative band in the short wavelength region, indicating a strong tilt of the porphyrin's x and y transition moments. As the complex stabilized, the magnitude of the LD^r in the Soret region increased but the shape remained. The overall shape of the LD^r spectrum in the entire wavelength region at the final stage was identical with that of the porphyrin 4–poly[d(A-T)$_2$] complex.

4. Discussion

4.1. Binding mode of porphyrin monomer 4 to DNA, poly[d(G-C)$_2$], and poly[d(A-T)$_2$]

As was mentioned in the Results section, the spectral properties of porphyrin 4 complexed with DNA, poly[d(A-T)$_2$], and poly[d(G-C)$_2$] are essentially the same as TMPyP complexed with the corresponding polynucleotide [10–12,17,18], indicating that the binding modes of porphyrin 4 are not different from those of TMPyP in spite of the substitution of one pyridiniumyl group with one functionalized phenyl ring. When associated with DNA, porphyrin 4 exhibits an intermediate red shift and hypochroism. An apparent negative CD band in the Soret absorption region, which is similar to that of the poly[d(G-C)$_2$] complex, and wavelength-independent LD^r with its magnitude larger than DNA absorption region indicate that porphyrin 4 is intercalated between DNA base pairs. Porphyrin 4 exhibits similar spectral change upon binding to poly[d(G-C)$_2$] with a more pronounced red shift in the absorption spectrum, indicating that porphyrin 4 also intercalates between the base pairs of poly[d(G-C)$_2$]. However, the spectral properties of the porphyrin 4–poly[d(A-T)$_2$] complex, which is characterized by two positive CD bands and a strong wavelength-dependent LD^r in the Soret region, are completely different from the former two complexes. Two apparent positive CD bands and a very strong tilt of the porphyrin transition moment in the Soret region indicate that porphyrin 4 binds in or near the minor groove of poly[d(A-T)$_2$]. Although a small variation was observed for all three complexes, the nature of the spectral properties remained the same for at least several days (data not shown), indicating that the binding mode does not change with time.

4.2. Association of porphyrin dimer 3 to various polynucleotides

The fact that the absorbance of porphyrin 3 in the Soret region increased by changing the solvent from water to ethanol (data not shown) indicates that, at least in part, porphyrin moieties are stacked in aqueous solution. The spectral properties of the porphyrin 3–poly[d(G-C)$_2$] complex immediately after mixing can be summarized as: (1) a strong hypochroism and a red shift in the absorption spectrum; (2) a negative CD band in the Soret band; (3) a significantly smaller LD^r magnitude in the Soret band compared to that in the DNA absorption region; and (4) a decreased LD^r magnitude in the DNA absorption region compared to the porphyrin-free poly[d(G-C)$_2$]. The negative CD band has been considered a diagnostic for the intercalated porphyrin [12,20]. Bis-intercalation of bis-porphyrin with methylene linker has been reported [27]. However, strong tilt angles for both x and y transition moments immediately after mixing are against intercalative binding of porphyrin, in which the molecular plane of porphyrin is perpendicular relative to the DNA helix axis—thereby, a large LD^r value is expected. This controversial observation can be solved by assuming that one of the porphyrin moiety intercalates while the other is free to rotate, thus it contributes to neither the LD nor CD in the initial complex. This assumption is supported by an increase in the negative CD and LD^r intensity as time lapsed. The final intensity of the negative CD is twice higher as the initial complex and the LD^r magnitude in the Soret band of the final complex is comparable to that in the DNA absorption region, indicating that the second porphyrin moiety intercalates slowly. Conceivably, the DNA stem is bent as a result of the first porphyrin intercalation because the LD^r magnitude in the DNA absorption region significantly decreases upon porphyrin 3 binding. However, the second intercalation does not result in further bending the DNA stem. We believe that the two porphyrin moieties in porphyrin 3 are stacked in aqueous solution because the absorbance and fluorescence intensity of porphyrin 3 increase at a higher temperature and in ethanol (data not shown). Therefore, the driving force for the first porphyrin intercalation may be large enough to overcome the stacking energy of the porphyrin moieties.

In the porphyrin 3–poly[d(A-T)$_2$] complex case, a relatively small red shift and a small decrease in the absorption spectrum, a bisignate CD, and a strong wavelength dependence in the LD^r spectrum are apparent immediately after mixing. All these spectral changes are consistent with porphyrin stacking outside of poly[d(A-T)$_2$] [11,12,15,16]. In the complex, some rearrangement of the porphyrin occurs, which results in a small shift in the maximum, an increase in the magnitude of the excitonic CD spectrum, and an increase in the LD^r magnitude both in DNA absorption and Soret regions. This observation conceivably reflects the idea that one of the stacked porphyrin dimers associates with poly[d(A-T)$_2$] at the initial stage, then the second

stacked dimer associates and stacks near the first dimer. This conclusion is supported by the fact that the intensity of excitonic CD increases without a lot of alteration of shape. This stacking of porphyrin dimer results in a rearrangement such that either one of the transition moments becomes close to that perpendicular to the DNA helix axis. Porphyrin stacking has recently been shown to occur in the major groove of the polynucleotide [18]. It should be noted that some bis-porphyrins in which two porphyrins are linked by a methylene chain exhibited bisignate CD when associated with poly[d(A-T)$_2$], while a negative CD band was apparent when complexed with poly(dA)·poly(dT) [26].

The spectral properties of the porphyrin 3–DNA complex at the final stage are characterized by: (1) a hypochroism and red shift in absorption; (2) a negative CD in the Soret region and a small but not negligible positive contribution in the 410– 420 nm range; (3) a negative LD^r signal in the Soret region, whose magnitude is comparable to that of the DNA absorption region; and (4) a decreased LD^r signal in the DNA absorption region compared to that of the porphyrin-free DNA. All these results indicate that the majority of the porphyrin components are intercalated to the base pairs. At the intercalation site, the DNA is locally bent, which is in contrast with the classical intercalators such as ethidium. However, part of the porphyrin is conceivably bound at the groove (without stacking), which is suggested by the positive portion at the short wavelength in the Soret band and some positive contributions in the LD^r around 430 nm. Positive contributions in the LD^r spectrum may be understood as a strong tilt of the transition moment of porphyrin with respect to the DNA helix axis.

Acknowledgements

This study was supported by the Korean Research Foundation (grant no. KRF-2002-070-C00053).

References

[1] R.J. Fiel, Porphyrin–nucleic acid interactions: a review, J. Biomol. Struct. Dyn. 6 (1989) 1259–1294.
[2] L.G. Marzilli, Medical aspects of DNA–porphyrin interactions, New J. Chem. 14 (1990) 409–420.
[3] R.F. Pasternack, E.J. Gibbs, in: A. Sigel, H. Sigel (Eds.), Metal Ions in Biological Systems, Porphyrin and Metalloporphyrin Interactions with Nucleic Acids, vol. 33, Marcel Dekker, New York, 1996, pp. 367–397.
[4] R. Kuroda, E. Takahashi, C.A. Austin, L.M. Fisher, DNA-binding and intercalation by novel porphyrins: role of charge and substituents probed by DNAse-I footprinting and topoisomerase-I unwinding, FEBS Lett. 262 (1990) 293–298.
[5] L.G. Marzilli, G. Pethö, M. Lin, M.S. Kim, D.W. Dixon, Tentacle porphyrins: DNA interactions, J. Am. Chem. Soc. 114 (1992) 7575–7577.
[6] R. Kuroda, H. Tanaka, DNA–porphyrin interactions probed by induced CD spectroscopy, J. Chem. Soc. Chem. Commun. (1994) 1575–1576.
[7] U. Sehlstedt, S.K. Kim, P. Carter, J. Goodisman, J.F. Vollano, B. Nordén, J.C. Dabrowiak, Interaction of cationic porphyrins with DNA, Biochemistry 33 (1994) 417–426.
[8] H.-J. Schneider, M. Wang, DNA interactions with porphyrins bearing ammonium side chains, J. Org. Chem. 59 (1994) 7473–7478.
[9] L.A. Lipcomb, F.X. Zhou, S.R. Presnell, R.J. Woo, M.E. Peek, R.R. Plaskon, L.D. Williams, Structure of a DNA–porphyrin complex, Biochemistry 35 (1996) 2818–2823.
[10] B.H. Yun, S.H. Jeon, T.-S. Cho, S.Y. Yi, U. Sehlstedt, S.K. Kim, Binding mode of porphyrins to poly[d(A-T)$_2$] and poly[d(G-C)$_2$], Biophys. Chem. 70 (1998) 1–10.
[11] S. Lee, Y.-A. Lee, H.M. Lee, J.Y. Lee, D.H. Kim, S.K. Kim, Rotation of the periphery methylpyridine of *meso*-tetrakis(*n*-*N*-methylpyridiumyl)porphyrin (*n*=2,3,4) and its selective binding to native and synthetic DNAs, Biophys. J. 83 (2002) 371–381.
[12] Y.-A. Lee, S. Lee, T.-S. Cho, C. Kim, S.W. Han, S.K. Kim, Binding mode of *meso*-tetrakis(*N*-methylpyridium-4-yl)porphyrin to poly[d(I-C)$_2$]: effect of amino group at the minor groove of poly[d(G-C)$_2$] on the porphyrin–DNA interaction, J. Phys. Chem., B 106 (2002) 11351–11355.
[13] J.S. Trommel, L.G. Marzilli, Synthesis and DNA binding of novel water-soluble cationic methylcobalt porphyrins, Inorg. Chem. 40 (2001) 4374–4383.
[14] R.F. Pastenack, S. Ewen, A. Rao, A.S. Meyer, M.A. Freedman, P.J. Collings, S.L. Frey, M.C. Ranen, J.C. de Paula, Interaction of copper(II) porphyrins with DNA, Inorg. Chim. Acta 317 (2001) 59–71.
[15] N.E. Mukundan, G. Pethö, D.W. Dixon, M.S. Kim, L.G. Marzilli, Interactions of an electron-rich tetracationic tentacle porphyrin with calf thymus DNA, Inorg. Chem. 33 (1994) 4676–4687.
[16] N.E. Mukundan, G. Pethö, D.W. Dixon, L.G. Marzilli, DNA–tentacle porphyrin interactions: AT over GC selectivity exhibited by an outside binding self-stacking porphyrin, Inorg. Chem. 34 (1995) 3677–3687.
[17] S. Lee, S.H. Jeon, B.-H. Kim, S.W. Han, H.G. Jang, S.K. Kim, Classification of CD and absorption spectra in the Soret band of H_2TMPyP bound to various synthetic polynucleotides, Biophys. Chem. 92 (2001) 35–45.
[18] Y.-A. Lee, J.-O. Kim, T.-S. Cho, R. Song, S.K. Kim, Binding mode of *meso*-tetrakis(*N*-methylpyridium-4-yl)porphyrin to AT regions: evidence for the porphyrin stacking in the major groove, J. Am. Chem. Soc. 125 (2003) 8107–8196.
[19] C. Casas, B. Saint-Jalmes, C. Loup, C.J. Lacey, B. Meunier, Synthesis of cationic metalloporphyrin precursors related to the design of DNA cleavers, J. Org. Chem. 58 (1993) 2913–2917.
[20] M.A. Ismail, P.M. Rodger, A. Rodger, Drug self-assembly on DNA: sequence effects with *trans*-bis(4-*N*-methylpyridiumyl)diphenyl porphyrins and Hoechst, J. Biomol. Struct. Dyn. Conversation 11 (2000) 335–348.
[21] X.W. Hui, N. Gresh, B. Pullman, Modelling of the binding specificity in the interactions of cationic porphyrins with DNA, Nucleic Acids Res. 18 (1990) 1109–1114.
[22] B. Nordén, M. Kubista, T. Kurucsev, Linear dichroism spectroscopy of nucleic acids, Q. Rev. Biophys. 25 (1992) 51–170.
[23] B. Nordén, T. Kurucsev, Analysing DNA complexes by circular and linear dichroism, J. Mol. Recognit. 7 (1994) 141–156.
[24] Y. Matsuoka, B. Nordén, Linear dichroism spectroscopy of nucleic acids, Biopolymers 22 (1983) 1713–1734.
[25] B. Härd, B. Nordén, Enantioselective interactions of inversion-labile trigonal iron[II] complexes upon binding to DNA, Biopolymers 25 (1986) 1209–1228.
[26] B. Nordén, S. Seth, Critical aspects of measurement of circular and linear dichroism; a device for absolute calibration, Appl. Spectrosc. 39 (1985) 647–655.
[27] H. Okada, H. Imai, Y. Uemori, Intercalation of water-soluble bis-porphyrins into poly(dA)–poly(dT) double helix, Bioorg. Med. Chem. 9 (2001) 3301–3307.